arXiv:1405.7133v2 [nucl-th] 16 Jun 2014

Testing in-medium πN dynamics on pionic atoms

E. Friedman[a,*], A. Gal[a]

[a] *Racah Institute of Physics, The Hebrew University, 91904 Jerusalem, Israel*

Abstract

A general algorithm for handling the energy dependence of meson-nucleon amplitudes in the nuclear medium has been recently applied to antikaons and to eta mesons. Here we test this approach on πN amplitudes in pionic atoms where direct comparison can be made with ample experimental results. Applying this algorithm to a large-scale fit of 100 pionic-atom data points across the periodic table, which also include the 'deeply-bound' states in Sn and Pb, reaffirms earlier conclusions on the density-dependent renormalization of the πN threshold isovector amplitude b_1, or equivalently the renormalization of the pion decay constant f_π in the nuclear medium.

Keywords: pion-nucleon in-medium interaction, energy dependence, pionic atoms

1. Dedication

This contribution is dedicated to the memory of Gerry Brown who has charted and shaped up the frontiers of Nuclear Physics for half a century. Gerry commissioned our two past reviews on exotic atoms [1, 2], realizing the potential of exotic atoms to provide hints and constraints on chiral signatures in dense matter. A brief update of our work on exotic atoms appeared in the 85th birthday Festschrift in honor of Gerald E Brown, *From Nuclei to Stars*, published in 2011 [3]. Here we revisit pionic atoms, a subject to which he made significant contributions in the 1970s.

*Corresponding author: E. Friedman, elifried@cc.huji.ac.il

2. Introduction

It was recognised in the early 1970s that the $\bar{K}$-nucleus interaction near threshold is determined by the $\bar{K}$-nucleon scattering amplitude at subthreshold energies [4, 5, 6]. The proximity of the $\Lambda(1405)$ resonance makes the $\bar{K}$-nucleus interaction quite sensitive to the proper description of the subthreshold region. An algorithm devised to account for the subthreshold energy dependence of the meson-nucleon amplitude in evaluating the meson-nucleus strong-interaction potential in kaonic atoms and for strongly-bound $\bar{K}$ mesons was formulated recently [7, 8, 9, 10, 11]. It has been employed in extensive calculations using several models for $\bar{K}$-nucleon scattering amplitudes that respect the recent SIDDHARTA results for kaonic atoms of hydrogen [12]. Another application of the same algorithm was made very recently in calculations of strongly-bound states of η mesons in nuclei [13, 14]. Here the proximity of the $N^*(1535)$ resonance enhances the sensitivity to the models used for the η-nucleon interaction and to the way the subthreshold region is handled. For an up-to-date overview of applications to in-medium $\bar{K}$ and η mesons, see Ref. [15].

In the two examples mentioned above no direct comparison with experiment could be made. Although there exists a reasonably broad database of strong interaction effects in kaonic atoms, the above approach is limited to K^- interactions with a single in-medium nucleon. Comparison with experiments gave evidence for a sizable component of the K^--nucleus potential which represents multinucleon interactions [9, 11] thus limiting one's ability to directly confront the model with experiment. Similarly, there is no experimental information on strongly bound antikaons in nuclei, nor any accepted direct evidence for bound η nuclear states.

Pion-nucleus interactions near threshold present a different scenario with respect to the above examples. No resonances are known near threshold and the real part of the pion-nucleus potential, which is part of the subthreshold algorithm, is dominated by single-nucleon interaction terms closely approximated by their free-space counterparts. Relatively small contributions arise from absorption on two nucleons which gives rise to the imaginary part of the potential. Moreover, the experimental database for pionic atoms is the most extensive of all exotic atoms [1, 2]. It is natural then to test the subthreshold approach by analysing pionic atom data where direct comparison with experiment is meaningful. On the other hand, owing to the rather smooth energy dependence of the free-space πN interaction, such tests may not prove

sufficiently sensitive to the fine details of the in-medium πN interaction even though they do provide acceptable support for the validity of the algorithm. It is therefore encouraging that the fits to pionic atom data reported here do preserve and even somewhat improve the existing level of agreement with the data, reaffirming earlier conclusions on the in-medium renormalization of the πN interaction [16, 17, 18, 19, 20, 21, 22, 23, 24, 25, 26, 27].

In Section 3 we present the model behind the algorithm for handling subthreshold pion-nucleon amplitudes in the medium. Results of global fits to pionic atom data are presented in Section 4, based on empirical energy-dependence of the pion-nucleon amplitudes. The in-medium enhancement of the πN isovector s-wave amplitude b_1 that received attention in the last two decades is examined and the role of the $E \to E - V_c$ 'minimal substitution' requirement is discussed. A summary and discussion are given in Section 5.

3. Subthreshold model

Here we briefly review the methodology of hadronic-atom calculations, using energy-dependent optical potentials within a suitably constructed subthreshold model.

3.1. Wave equation

Starting from a meson Klein-Gordon (KG) equation, the dispersion relation corresponding to a meson of mass m, momentum $\vec{p}$ and energy E in nuclear medium of density ρ is traditionally written as [2]

$$E^2 - \vec{p}^{\,2} - m^2 - \Pi(E, \vec{p}, \rho) = 0, \tag{1}$$

in terms of a self energy (polarization operator) $\Pi(E, \vec{p}, \rho)$. Introducing the meson-nuclear optical potential $V_{\rm opt}$ by $\Pi(E, \vec{p}, \rho) = 2EV_{\rm opt}$, the following KG equation is obtained for finite nuclei and at or near threshold:

$$\left[\nabla^2 - 2\mu(B + V_{\rm opt} + V_c) + (V_c + B)^2\right]\psi = 0, \tag{2}$$

where $\hbar = c = 1$ was implicitly assumed in these equations. Here μ is the meson-nucleus reduced mass, B is the complex binding energy, V_c is the finite-size Coulomb interaction of the meson with the nucleus, including vacuum-polarization terms, all added according to the minimal substitution principle $E \to E - V_c$. $V_{\rm opt}$ is the optical potential of the meson in the

medium. Additional terms $2V_cV_{\rm opt}$ and $2BV_{\rm opt}$ were neglected in Eq. (2) with respect to $2\mu V_{\rm opt}$.

For pions, the emphasis in past studies of medium effects has been on the density dependence of the self energy operator $\Pi(E,\vec{p},\rho)$, or equivalently of the optical potential $V_{\rm opt}$. The density dependence of $V_{\rm opt}$ is briefly reviewed in Section 3.2 below, while the energy and momentum dependence, which is the focus of the present work, is studied in Section 3.4.

3.2. Pion-nucleus potential

The zeroth-order optical potential $V_{\rm opt}^{(0)} = t\rho$ is linear in the density ρ, with t the free-space meson-nucleon t matrix. This optical potential is real at zero energy because pions cannot be absorbed at rest by a single nucleon, although they can be absorbed by the nucleus. Ericson and Ericson [28] introduced ρ^2 terms into the potential to describe schematically π^- absorption on pairs of nucleons. The π^- optical potential then becomes

$$2\mu V_{\rm opt}(r) = q(r) + \vec{\nabla}\cdot\alpha(r)\vec{\nabla}, \tag{3}$$

with its s-wave part $q(r)$ given by

$$\begin{aligned} q(r) &= -4\pi(1+\frac{\mu}{m_N})\{\overline{b}_0[\rho_n(r)+\rho_p(r)] + \overline{b}_1[\rho_n(r)-\rho_p(r)]\} \\ &\quad -4\pi(1+\frac{\mu}{2m_N})4B_0\rho_n(r)\rho_p(r), \end{aligned} \tag{4}$$

where ρ_n and ρ_p are the neutron and proton density distributions normalized to the number of neutrons N and number of protons Z, respectively, and m_N is the mass of the nucleon. The p-wave part of the potential, $\alpha(r)$, is effective only near the nuclear surface and will not be further discussed here; it is used in the present work in the same way as in Ref. [2]. The coefficients $\overline{b}_0$ and $\overline{b}_1$ are *effective*, implicitly density-dependent pion-nucleon isoscalar and isovector s-wave scattering amplitudes evolving from the free-space amplitudes b_0 and b_1, respectively, and are essentially real near threshold. The parameter B_0 represents multi-nucleon absorption and therefore has an imaginary part. The real part of B_0 stands for dispersive contributions which could play a role in pionic atoms.

The free-space values of the isoscalar and isovector πN center-of-mass (cm) scattering amplitudes at threshold are known from pionic hydrogen and deuterium X-ray measurements [29]

$$b_0 = -0.0001^{+0.0009}_{-0.0021}\, m_\pi^{-1}, \qquad b_1 = -0.0885^{+0.0010}_{-0.0021}\, m_\pi^{-1}. \tag{5}$$

A recent chiral perturbation calculation of the $\pi^- d$ scattering amplitude, reanalysing these X-ray measurements, finds the following values [30]:

$$b_0 = 0.0076 \pm 0.0031\ m_\pi^{-1}, \qquad b_1 = -0.0861 \pm 0.0009\ m_\pi^{-1}. \tag{6}$$

One notes the close agreement between the two determinations of b_1 whereas the values of b_0, accepting the quoted uncertainties, disagree with each other. Yet, these values of b_0 and b_1 are well approximated by the Tomozawa-Weinberg (TW) lowest-order chiral limit [31]

$$b_0 = 0, \qquad b_1 = -\frac{\mu_{\pi N}}{8\pi f_\pi^2} = -0.079\ m_\pi^{-1}. \tag{7}$$

Since the value of the amplitude b_0 from Eqs. (5)-(6) is exceptionally small, it is mandatory to include double-scattering contributions in the construction of the isoscalar single-nucleon term in $q(r)$, giving rise to explicit density dependence for Pauli correlated nucleons [32]

$$\overline{b}_0 = b_0 - \frac{3}{2\pi}(b_0^2 + 2b_1^2)p_F, \tag{8}$$

where p_F is the local Fermi momentum corresponding to the local nuclear density $\rho = 2p_F^3/(3\pi^2)$. Here b_1^2 contributes significantly to $\overline{b}_0$, thereby making the isovector amplitude b_1 effective also in $N = Z$ pionic atoms. The TW expression (7) for b_1 suggests that its in-medium renormalization is directly connected to that of the pion decay constant f_π, given to first order in the nuclear density ρ by [33, 34]

$$\frac{f_\pi^2(\rho)}{f_\pi^2} = \frac{<\bar{q}q>_\rho}{<\bar{q}q>_0} \simeq 1 - \frac{\sigma\rho}{m_\pi^2 f_\pi^2}, \tag{9}$$

where $<\bar{q}q>_\rho$ stands for the in-medium chiral condensate and $\sigma \simeq 50$ MeV is the pion-nucleon σ term. Extending Eq. (7) for b_1 from free space to dense matter, this leads to the following density dependence for the in-medium b_1:

$$b_1(\rho) = \frac{b_1}{1 - \sigma\rho/m_\pi^2 f_\pi^2} = \frac{b_1}{1 - 2.3\rho} \tag{10}$$

with ρ in units of fm^{-3}. In this model, introduced first by Weise [33, 34], the explicitly density-dependent $b_1(\rho)$ of Eq. (10) replaces the effective isovector coefficient $\overline{b}_1$ in the pion-nucleus s-wave potential $q(r)$ of Eq. (4). This has been referred to in the literature as a necessary signature of partial restoration of chiral symmetry in dense matter. We note that the linear density approximation introduced in Eq. (9) provides an excellent representation of quark condensate effects at densities below nuclear matter density [35].

3.3. Nuclear densities

An important ingredient in the analysis of pionic atoms are the nuclear densities to be used in the potential (3). With proton densities considered known we scan over neutron densities searching for a best agreement with the data. A linear dependence of $r_n - r_p$, the difference between the root-mean-square (rms) radii, on the neutron excess ratio $(N-Z)/A$ has been accepted as a useful quantity, parameterized as

$$r_n - r_p = \gamma \frac{N-Z}{A} + \delta \ , \tag{11}$$

with γ close to 1.0 fm and δ close to zero. Two-parameter Fermi distributions are used for ρ_n with the same diffuseness parameter as for the protons, the so-called 'skin' shape [2, 36] which was found to yield lower values of χ^2 for pions.

3.4. Energy dependence

The model underlying the subthreshold algorithm adopts the Mandelstam variable $s = (E_\pi + E_N)^2 - (\vec{p}_\pi + \vec{p}_N)^2$ as the argument transforming free-space to in-medium pion-nucleon amplitudes, where both the pion and the nucleon variables are determined independently by the respective environment of a pionic atom and a nucleus. Consequently, unlike in the two-body cm system, here $\vec{p}_\pi + \vec{p}_N$ does not vanish, and one gets $(\vec{p}_\pi + \vec{p}_N)^2 \to p_\pi^2 + p_N^2$ upon averaging over angles. The energies are given by

$$E_\pi = m_\pi - B_\pi, \qquad E_N = m_N - B_N, \tag{12}$$

where B are binding energies and m are masses. For the pion momentum we substitute locally

$$\frac{p_\pi^2}{2m_\pi} = -B_\pi - \mathrm{Re}\ V_{\mathrm{opt}} - V_c \tag{13}$$

with V_{opt} the pion-nucleus optical potential and V_c the pion Coulomb potential due to the finite-size nuclear charge distribution. For the nucleon we adopt the Fermi gas model (FGM), yielding in the local density approximation

$$\frac{p_N^2}{2m_N} = T_N\ (\rho/\bar{\rho})^{2/3}, \tag{14}$$

where ρ is the local density, $\bar{\rho}$ the average nuclear density and T_N is the average nucleon kinetic energy which assumes the value 23 MeV in the FGM.

This value, used here, is larger than that derived from shell-model calculations across the periodic table (18.4 MeV in ^{208}Pb), but smaller than that derived in many-body approaches (38.2 MeV in ^{208}Pb), see Tables I and II in Ref. [37]. Most of the difference between these two groups of values is believed to arise from short-range nuclear correlations at the high density regime which is inaccessible in exotic atoms. For this reason, furthermore, we kept only the leading density power 2/3 in Eq. (14).

Defining $\delta\sqrt{s} = \sqrt{s} - E_{\rm th}$ with $E_{\rm th} = m_\pi + m_N$, then to first order in $B/E_{\rm th}$ and $(p/E_{\rm th})^2$ one gets

$$\delta\sqrt{s} = -B_N\rho/\bar{\rho} - \xi_N[T_N(\rho/\bar{\rho})^{2/3} + B_\pi\rho/\rho_0] + \xi_\pi[{\rm Re}\ V_{\rm opt} + V_c(\rho/\rho_0)^{1/3}], \quad (15)$$

with $\xi_N = m_N/(m_N + m_\pi)$, $\xi_\pi = m_\pi/(m_N + m_\pi)$, and $\rho_0 = 0.17$ fm^{-3}. Following previous applications [7, 8, 9, 10, 11] an average binding energy value of $B_N = 8.5$ MeV is used. The specific ρ/ρ_0 and $\rho/\bar{\rho}$ forms of density dependence ensure that $\delta\sqrt{s} \to 0$ when $\rho \to 0$ [11].

Another variant of Eq. (15) is obtained when considering the minimal substitution requirement, the importance of which for incorporating electromagnetism in a gauge-invariant way into the pion optical potential was first pointed out by Ericson and Tauscher [38] and more recently emphasized by Kolomeitsev, Kaiser and Weise [20]. Indeed, the application of minimal substitution has been successful in analyses of pionic atoms [2, 24] and pion scattering at low energies [27]. Here $E = E_\pi + E_N$ is replaced by $E - V_c$ and then Eq. (15) becomes

$$\delta\sqrt{s} = -B_N\rho/\bar{\rho} - \xi_N[T_N(\rho/\bar{\rho})^{2/3} + B_\pi\rho/\rho_0 + V_c(\rho/\rho_0)^{1/3}] + \xi_\pi{\rm Re}\ V_{\rm opt}. \quad (16)$$

Equations (15)-(16) show that the subthreshold energies where the πN amplitudes in $V_{\rm opt}$ are to be evaluated depend, locally, on the optical potential $V_{\rm opt}$ which, according to Eqs. (3)-(8), depends on these amplitudes. Therefore these equations have to be solved *self-consistently*, a process that is found to converge after 4–6 iterations which are done at every radial point for the local value of the nuclear density ρ. This process defines a density-to-energy transformation which makes the potential density dependent, in addition to any genuine density dependence of the πN amplitudes. Only the s-wave term of the potential, $q(r)$, is used by us to calculate the subthreshold energies in pionic atoms, as the p-wave term, $\alpha(r)$, is effective primarily near the nuclear surface.

Figure 1 shows examples of the density-to-energy transformation for three pionic atoms in comparison with typical results for kaonic atoms, with $\delta\sqrt{s}$

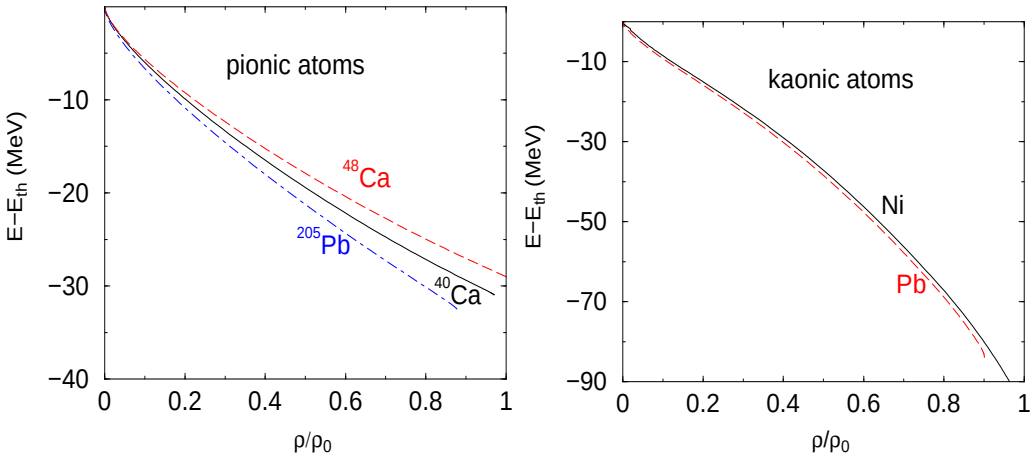

Figure 1: Examples of the density-to-energy transformation in pionic atoms (left panel) and in kaonic atoms (right panel, from [11]) using Eq. (15) for pionic atoms and its obvious adjustment for kaonic atoms.

denoted by $E - E_{\rm th}$. Note that the example of pionic atom of ^{205}Pb is an extreme case as it relates to a deeply bound $2p$ pionic state with a very large binding energy of close to 6 MeV. The empirical πN scattering amplitudes used, including their energy dependence, were taken from πN phase shifts derived from the SAID program [39], yielding a slope of $-0.00053 m_\pi^{-1}$/MeV for b_0. We use this slope also below threshold. For b_1, its variation with energy is negligibly small and therefore ignored here. The figure demonstrates clearly that subthreshold energies of order -20 MeV, at $\rho_0/2$, are encountered in pionic atoms (left panel). Although smaller than typically -40 MeV in kaonic atoms (right panel), this constitutes a nonnegligible effect. The difference between pionic and kaonic atoms originates from the very different meson-nuclear s-wave potentials for these two systems. For K^-, with attractive real part of the potential, the energy shift $\delta\sqrt{s}$ is negative definite when disregarding the minimal substitution contribution. For pions, the real part of the s-wave potential is repulsive but, nevertheless, $\delta\sqrt{s}$ is negative due to the dominance of the $-p^2$ contributions in the expression for the Mandelstam energy variable s. The significance of these momentum-dependent contributions precludes relating to pions in finite nuclei as zero-momentum pions, a term used often for pions in nuclear matter.

4. Results

In studying the model for handling pion-nucleon interactions in the nuclear medium we compare our new results with earlier analyses [2] where the interactions were either taken at threshold or effectively above threshold when adopting the minimal substitution principle. We therefore consider here, as in Ref. [2], global fits to 100 data points for strong interaction observables in pionic atoms, from Ne to U, including deeply bound pionic atoms of three Sn isotopes and of ^{205}Pb.

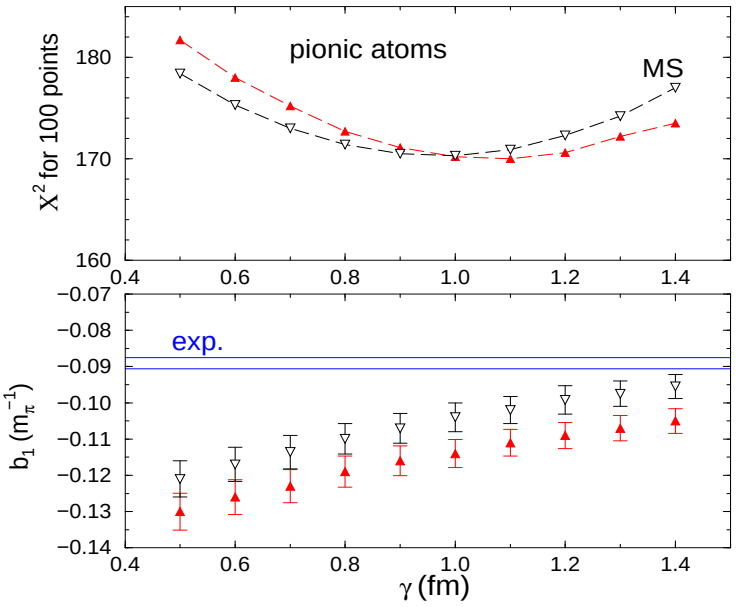

Figure 2: Results of fits for variable γ, the neutron rms radius parameter in Eq. (11), with b_1 not modified in the medium. Filled triangles up: $\delta\sqrt{s}$ from Eq. (15), opaque triangles down: including also minimal substitution (MS) as per Eq. (16). Also shown is the experimental value of b_1 at threshold [29].

The ability to perform least-squares fits to a broad data set for pionic atoms is a major difference between the present work and our earlier applications of the sub-threshold approach. For example, changing input parameters such as T_N in Eqs. (15)-(16) causes values of fit parameters to change too in order to maintain best agreement with the data. Replacing $\bar{\rho}$ by ρ_0 in the T_N term, for example, results in the parameter b_0 changing within error, to compensate for changes due to the T_N term. Most important is the

observation that changes in the isovector parameter b_1 are only 30% of their (rather small) uncertainties.

Figure 2 shows typical results of fits obtained when varying parameters of the pion-nucleus potential and scanning over the neutron rms radius parameter γ, for a fixed value of $\delta = -0.035$ fm, see Eq. (11). Finite-range folding in the p-wave term is included as before [2]. A shallow minimum determines γ to be around 1.0±0.15 fm, in full agreement with a multitude of other results [36, 40]. For a check, we note that the value obtained from Eq. (11) for ^{208}Pb is $r_n - r_p$=0.18±0.03 fm, in agreement with more direct recent derivations [41, 42].

Table 1: Values of B_0 (m_π^{-4} units) obtained in large-scale pionic-atom fits, with minimal substitution (MS) disregarded (No) or employed (Yes), using the subthreshold energy algorithms (15) and (16) respectively, with (Yes) or without (No) Weise's renormalization ansatz (10).

MS/Weise	No/No	No/Yes	Yes/No	Yes/Yes
$-$Re B_0	0.112±0.031	0.040±0.032	0.076±0.032	0.012±0.033
Im B_0	0.052±0.002	0.051±0.002	0.052±0.002	0.052±0.002

Focusing on the isovector s-wave parameter b_1, it is seen from Fig. 2 that when it is not modified in the medium, other than by the subthreshold energy algorithm (15), it turns out to be too repulsive by 5-6 error bars compared to the free pion-nucleon experimental value. When minimal substitution is imposed as per Eq. (16), the discrepancy becomes slightly smaller but, nevertheless, the so-called b_1 anomalous enhancement is observed. These conclusions are in agreement with earlier work not using the subthreshold energy algorithm.

The possibility that b_1 is enhanced in the nuclear medium was put forward by Weise [33, 34], see Eq. (10). This ansatz is supported by experiments both below threshold [16, 17] and above [26, 27]. Figure 3 shows that the best χ^2 is now 4-5 units smaller than without this explicit density dependence of $b_1(\rho)$ and the values of the free-space b_1 from the fit agree with the known free value, with a hint that the agreement is better when minimal substitution is applied. Another indication in favor of combining the renormalization ansatz (10) together with minimal substitution $E \to E - V_c$ is provided by inspecting the values obtained in our large-scale pionic-atom fits for the two-nucleon parameter B_0 of Eq. (4), as shown in Table 1. It is seen that

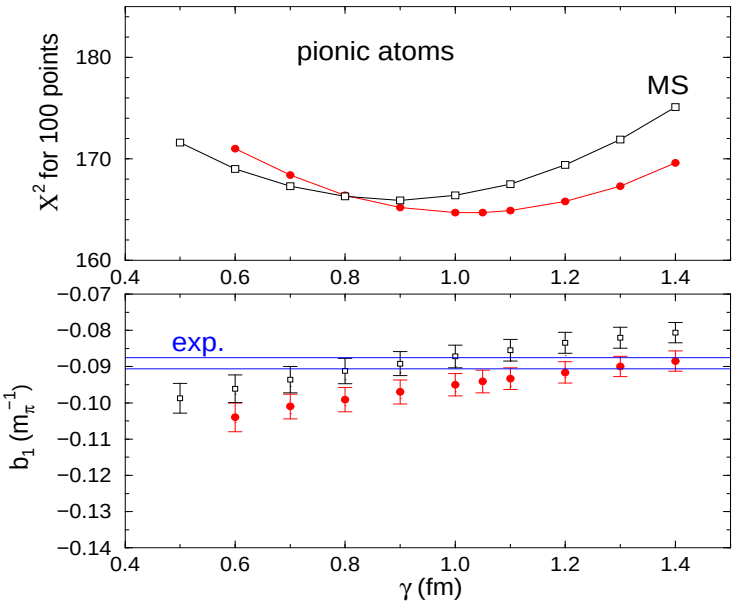

Figure 3: Results of fits for variable γ, the neutron rms radius parameter in Eq. (11), with $b_1(\rho)$ given by Eq. (10). Filled: $\delta\sqrt{s}$ from Eq. (15), opaque: including also minimal substitution (MS) as per Eq. (16). The free-space threshold value of b_1 [29] is also shown.

the value of Im B_0 is determined in great precision and is insensitive to the variants used. In contrast, the fitted value of Re B_0 is sensitive to these variants and it also emerges with a fairly large uncertainty which, however, is independent of the variant used. Anticipating values of Re B_0 smaller or equal in magnitude to Im B_0, the fitted values listed in the table give preference to accepting both the minimal-substitution principle and Weise's renormalization ansatz [33, 34].

5. Summary and discussion

We have presented in this update global analyses of strong interaction effects in pionic atoms, where the algorithm applied recently [15] in other systems for handling meson-nucleon in-medium interactions near threshold is tested. This approach defines energy scale of ≈20 MeV over which the πN s-wave amplitudes contribute to the pion-nucleus interaction. These energies are below threshold when minimal substitution is disregarded, but part of

the energy range can be above threshold when minimal substitution is maintained. In all previous analyses, before introducing these algorithms, the πN energy was either on threshold when minimal substitution was disregarded, or fully above threshold when respecting minimal substitution. Nevertheless, the overall conclusions are practically the same whether or not the present algorithms are applied. In particular, the lowest χ^2 implies a value of χ^2 per degree of freedom of about 1.7 and is obtained for rms radii of neutron distributions that agree with those deduced by other methods. The best-fit b_1 values agree with the free pion-nucleon value only when explicit density-dependence of b_1 as suggested by Weise [33, 34] is incorporated. These results were obtained using the SAID empirical energy dependence of b_0, as distinct from the chiral-model energy dependence evaluated for zero-momentum pions. We refer the reader to our earlier discussion of this point [24] adding that pions have appreciable momentum within the nuclear interior, as given by Eq. (13).

The low sensitivity revealed in the present work results from the smooth dependence on energy of the empirical b_0 parameter. Considering the energy at which b_0 is calculated, and assuming an average effective density of 50-60% of the central density [18, 19], then the respective energy differences between any previous analysis and its present counterpart are around 20 MeV. With an empirical b_0 slope of $-0.00053 m_\pi^{-1}$/MeV [39] a variation of 0.01 m_π^{-1} in b_0 values is implied, which is indeed produced in the respective χ^2 fits. Furthermore, with b_1 essentially independent of energy, the variations in b_0 translate to these same variations in $\overline{b}_0$. This $\approx$0.01 m_π^{-1} variation in b_0 is also consistent with the uncertainty placed on it in the SAID partial-wave analysis [39]. This somewhat trivial result is, nevertheless, reassuring in supporting the viability of the subthreshold algorithm.

Finally we comment that the results and conclusions reached in the present update hold valid also when the 'deeply bound' states (DBS) in ^{205}Pb and in ^{115,119,123}Sn are removed from the large-scale fits of pionic atoms described here. This agrees with earlier conclusions reached by us [3, 22, 23] where it was shown that the uncertainties in the derived value of b_1 from DBS, or from DBS plus $1s$ states in light $N = Z$ nuclei, are considerably larger than those derived from large-scale fits (about 0.004 m_π^{-1}, see Figs. 2 and 3). Other approaches considering only partial sets of pionic-atom data and claiming similar uncertainties, as reviewed in Ref. [43], ignore additional systematic uncertainties arising from fixing the p-wave πN potential $\alpha(r)$ in Eq. (3). We stress that our large-scale fits involve a comprehensive parameter

search, including the p-wave interaction parameters not discussed here. The few DBS established accurately so far are still short of providing *on their own* the necessary precision to substantiate the deduced renormalization of b_1 and the implied partial restoration of chiral symmetry in dense matter through the decrease of f_π, given to a good approximation by Eq. (9).

Acknowledgments

Special thanks are due to Wolfram Weise for many stimulating discussions on exotic atoms throughout the last two decades. This research was partly supported by the HadronPhysics3 networks SPHERE and LEANNIS of the European FP7 initiative.

References

[1] C.J. Batty, E. Friedman, A. Gal, Phys. Rep. 287 (1997) 385.

[2] E. Friedman, A. Gal, Phys. Rep. 452 (2007) 89.

[3] E. Friedman, A. Gal, in: Sabine Lee (Ed.), From Nuclei to Stars, World Scientific, 2011, pp.127-140.

[4] S. Wycech, Nucl. Phys. B 28 (1971) 541.

[5] W.A. Bardeen, E.W. Torigoe, Phys. Lett. B 38 (1972) 135.

[6] J.R. Rook, Nucl. Phys. A 249 (1975) 466.

[7] A. Cieplý, E. Friedman, A. Gal, D. Gazda, J. Mareš, Phys. Lett. B 702 (2011) 402.

[8] A. Cieplý, E. Friedman, A. Gal, D. Gazda, J. Mareš, Phys. Rev. C 84 (2011) 045206.

[9] E. Friedman, A. Gal, Nucl. Phys. A 881 (2012) 150.

[10] D. Gazda, J. Mareš, Nucl. Phys. A 881 (2012) 159.

[11] E. Friedman, A. Gal, Nucl. Phys. A 899 (2013) 60.

[12] M. Bazzi, et al., Phys. Lett. B 704 (2011) 113, Nucl. Phys. A 881 (2012) 88.

[13] E. Friedman, A. Gal, J. Mares, Phys. Lett. B 725 (2013) 334.

[14] A. Cieplý, E. Friedman, A. Gal, J. Mareš, Nucl. Phys. A 925 (2014) 126.

[15] A. Gal, E. Friedman, N. Barnea, A. Cieplý, D. Gazda, J. Mareš, Acta Phys. Pol. B 45 (2014) 673.

[16] P. Kienle, T. Yamazaki, Phys. Lett. B 514 (2001) 1, using preliminary results reported subsequently by H. Geissel, et al., Phys. Rev. Lett. 88 (2002) 122301.

[17] E. Friedman, Phys. Lett. B 524 (2002) 87.

[18] H. Geissel, et al., Phys. Lett. B 549 (2002) 64.

[19] T. Yamazaki, S. Hirenzaki, Phys. Lett. B 557 (2003) 20.

[20] E.E. Kolomeitsev, N. Kaiser, W. Weise, Phys. Rev. Lett. 90 (2003) 092501.

[21] E.E. Kolomeitsev, N. Kaiser, W. Weise, Nucl. Phys. A 721 (2003) 835c.

[22] E. Friedman, A. Gal, Nucl. Phys. A 721 (2003) 842c.

[23] E. Friedman, A. Gal, Nucl. Phys. A 724 (2003) 143.

[24] E. Friedman, A. Gal, Phys. Lett. B 578 (2004) 85.

[25] K. Suzuki, et al., Phys. Rev. Lett. 92 (2004) 072302.

[26] E. Friedman, et al., Phys. Rev. Lett. 93 (2004) 122302.

[27] E. Friedman, et al., Phys. Rev. C 72 (2005) 034609.

[28] M. Ericson, T.E.O. Ericson, Ann. Phys. 36 (1966) 323.

[29] H.-Ch. Schröder, et al., Eur. Phys. J. C 21 (2001) 473.

[30] V. Baru, C. Hanhart, M. Hofenrichter, B. Kubis, A. Nogga, D.R. Phillips, Phys. Lett. B 694 (2011) 473.

[31] Y. Tomozawa, Nuovo Cimento A 46 (1966) 707; S. Weinberg, Phys. Rev. Lett. 17 (1966) 616.

[32] M. Krell, T.E.O. Ericson, Nucl. Phys. B 11 (1969) 521.

[33] W. Weise, Acta Phys. Pol. B 31 (2000) 2715.

[34] W. Weise, Nucl. Phys. A 690 (2001) 98c.

[35] N. Kaiser, P. de Homont, W. Weise, Phys. Rev. C 77 (2008) 025204.

[36] E. Friedman, Hyperfine Interactions 193 (2009) 33.

[37] C. Ciofi degli Atti, S. Simula, Phys. Rev. C 53 (1996) 1689.

[38] T.E.O. Ericson, L. Tauscher, Phys. Lett. B 112 (1982) 425.

[39] SAID program gwdac.phys.gwu.edu, see R.A. Arndt, W.J. Briscoe, I.I. Strakovsky, R.L. Workman, Phys. Rev. C 74 (2006) 045205.

[40] J. Jastrzębski, et al., Int. J. Mod. Phys. E 13 (2004) 343.

[41] E. Friedman, Nucl. Phys. A 896 (2012) 46.

[42] C.M. Tarbert, et al. (Crystal Ball at MAMI and A2 Collaboration), arXiv:1311.0168.

[43] T. Yamazaki, S. Hirenzaki, R.S. Hayano, H. Toki, Phys. Rep. 514 (2012) pp. 1-87.